Calibration of a Meandering Simulation Model to the Yampa River

Alan D. Howard
Department of Environmental Sciences
University of Virginia
Charlottesville, VA 22903
(804) 924-0563
(804) 982-2137 (FAX)
ah6p@virginia.edu

May 27, 1997

The Yampa River near Hayden Colorado flows through a wide floodplain and, with the exception of short sections where the valley is narrow or where the channel impinges on valley walls, is freely meandering (Figure 1). The river is of modest sinuosity (ranging from about 1.7 in 1938 to about 1.4 in 1989). The channel has exhibited classic meandering by outer band erosion and point bar development during this period. Meandering channels that are subject to only neck cutoffs (when adjacent loops physically intersect) have a high sinuosity (> 3.0) (e.g., simulations in Howard, 1992). Both the restricted sinuosity and the record of channel pattern changes (Figures 1 and 2) indicate that chute cutoffs are the dominant mechanism that controls sinuosity.

As part of a project undertaken by the Nature Conservancy, the author has undertaken the task of calibrating a simulation model of stream meandering (Howard, 1992, 1996) to the Yampa River. The calibration consists of three parts, 1) estimating hydrologic and sedimentologic factors controlling meander migration; 2) calibration of a probabilistic chute cutoff model for the Yampa; and 3) relating simulation and natural timescales through selection of an appropriate bank erodibility. Details of the model are discussed in Howard (1992, 1996)[1], so that the only discussion of the model focuses on calibration issues.

Hydrologic and Sedimentologic Parameters: The flow and bed topography in the simulation model depends upon 5 parameters (Howard, 1992, Table 1.1):

β A parameter governing the cross-sectional slope in bends. A value of 2.5 is used in accord with recommendations of Ikeda et al. (1981), Johanneson and Parker (1989).

M An exponent relating velocity to bedload transport rate. A value of 3.0 is assumed.

F_0 Froude Number at bankfull discharge. This is estimated as 0.5 based upon the gradient of the Yampa River, observed bankfull depth, and observed bankfull discharge. Appropriate data was supplied by Christina Ostendorf.

γ_0 The bankfull width-depth ratio of the channel. Estimated to be 20.0 based upon cross sections surveyed by Christina Ostendorf.

C_f A measure of friction exerted by the bed and banks on the flow, and measured by the square of the ratio of shear velocity to mean velocity. This was initially estimated as 0.015 based upon the gradient of the Yampa River, observed bankfull depth, and observed bankfull discharge.

The pattern of meandering is only weakly dependent upon the parameters β, M, and F_0. The width-depth ratio, γ_0, is well constrained by measured cross-sections. The coefficient of friction, C_f, has a strong control over the wavelength of the simulated meandering and is rather poorly constrained by the existing data. Thus the approach that was taken was to fit C_f by comparison of the dominant wavelength of meandering of simulated planforms with that of the Yampa River. Several measures of dominant wavelength were defined by Howard and Hemberger (1991); these were used to make the comparison. The dominant wavelength is also affected by the frequency of chute cutoffs, and thus indirectly by the sinuosity. The values of C_f and cutoff probability (see below) were therefore determined through experimentation to produce a simulated meandering pattern with the appropriate sinuosity and wavelength. The resulting value of C_f is 0.02, which is very close to the value which was originally estimated.

Chute Cutoff Parameters: Howard (1996) introduced probabilistic chute cutoffs into the simulation model. The probability of chute development at a given time and across a given potential chute path is:

$$P = K_c R_c e^{(-K_d D_c - K_c E + K_a \cos\psi + K_v u_{lb})}$$

where

$$R_c = (D_p - D_c)/D_p = (\mu_c - 1)/\mu_c .$$

The gradient ratio R_c depends upon the relative distances (and hence also overall gradients) across the existing flowpath D_p amd acrpss the potential chute D_c, and it can also be expressed in terms of the cutoff sinuosity $\mu_c = D_p/D_c$. In evaluating this expression the downstream channel gradient is assumed to be uniform. The

terms in the exponential reflect the presumed smaller probablility of cutoff across longer chute lengths and floodplains with higher elevation, E (measured as the maximum elevation across the chute). Additionally, the probability of cutoff can be assumed to dectrease as the angle ψ between the existing flowpath and the cutoff path increases. Finally, the probability of cutoff is assumed to increase if the flow velocity (u_{1b}, the velocity perterbation) near the bank at the site of potential cutoff is high. The coefficents, K, are assumed to be temporally constant. The sum of the exponential terms is restricted to values ≤ 0. In the simulations here the coefficients K_e, K_a, and K_v are assumed to be zero, so that possible effects of elevation, velocity, and cutoff angle are not included.

Two patterns of cutoffs occur depending upon whether the probability of cutoffs decrease as the distance D_c increases for a given R_c, that is, whether the coefficient K_d is included or not. When the cutoffs are strongly conditioned by distance such that K_d is large, cutoffs are mostly short and across single meander necks. In addition, the sinuosity stays within a narrow range (Figure 3). However, if K_d is small or negligible, quite long chute cutoffs (or avulsions) can occur occasionally in areas of high sinuosity, and the total sinuosity undergoes large excursions through time (Figure 4). The large change of sinuosity during the period 1938 to the present (about 1.7 to 1.4) suggests the occurrence of long cutoffs, as does the observed pattern of cutoffs. In addition, simulated streams with occasional long cutoffs typically exhibit a pattern in which long, nearly straight reaches (at sites of recent avulsions) alternate with more sinuous reaches (Figure 5). All of these patterns suggest that long cutoffs occur on the Yampa River, and that cutoff distance, as controlled by K_d, is a small or negligible factor in cutoffs. Therefore, a series of simulations were run starting with the 1938 Yampa planform to select a value of K_c. Figures 6 through 8 show the evolution of sinuosity for simulations with various values of K_c; for each value there were 5 simulations seeded with different random numbers. A value of 0.02 (with the possibility of chute cutoffs evaluated every 50 iterations) was selected because the sinuosity generally stays in the range observed between 1938 and the present, and several cases show the initial rapid decline in sinuosity observed after 1938. Figures 9-13 show the temporal evolution of these five simulations for K_c =0.02 with different random seeds, showing the occasional occurrence of long cutoffs.

Calibration of Bank Erodibility. In the model bank erodibility is assumed to be unity, and the simulation occurs with an internal clock of simulated 'years'. To apply this in a predictive manner, this internal clock must be calibrated to the natural time scale. This was done by running the model from the 1938 planform and observing how close the simulated planform came to the 1987 planform as a function of simulation time. The measures that were used were the mean separation between the simulated planform and the 1987 planform and the standard deviation of that separation. Figure 14 shows the temporal evolution of that deviation, or error, for the simulations shown in Figures 9-13. Both the

mean error and standard deviation of the error reach a minimum at a simulation time of about 550, suggesting that 11.2 simulation 'years' equal one actual year.

Statistics from an Exploratory Simulation

Figure 5 shows representative channel centerlines during an example simulation with 10000 iterations corresponding to about 37,500 model 'years' and 3350 natural years (so that 3 iterations correspond to 1 natural year) which started from the 1938 channel planform. Figure 15 portrays the temporal variation in sinuosity. On each cell of the overall simulation domain the age, A, elevation, E, and distance from the nearest channel, X, was noted. Only cells through which the channel had migrated during the simulation are utilized in the analysis - other parts of the simulated floodplain domain were assumed to be indefinitely older and not included in the analysis. The data from this simulation are summarized in two figures. The number of cells of various lengths of time since the channel last occupied that cell were noted and are summarized as a cumulative frequency versus age in iterations in Figure 16. For example, about 50% of the floodplain cells were less than or equal to 3000 iterations (1000 years) in age. The count was tallied only to 4700 iterations, so that all cells older than this are included in the last point. Also shown on this figure is the mean floodplain elevation as a function of age (as noted below, the elevation characteristics of the floodplain were not calibrated as part of this project).

Figure 17 shows the cumulative number of cells, mean age, and mean floodplain elevation as a function of distance from the active channel at the close of the simulation (zero data points at 1200 and 1250 meters represent no information rather than actual zero values). Distance is scaled to the Yampa River dimensions, so that distance is in meters.

Conclusions and Discussion

Calibration of a floodplain similation model improves the longer the record of observation, the longer the section of river that has available data, and the better the information on river hydraulics and floodplain elevations. The database for the Yampa River is far from ideal in this respect. The situation is made more uncertain because of the low sinuosity of the river and the dominance of chute cutoffs. Observations of chute cutoffs in natural rivers are sparse, and one can place little confidence in the details of the formulation of the probabilistic model utilized here. Chute cutoffs always involve a strong dependency upon flood history and the detailed morphology of the local site of potential cutoffs - unlike neck cutoffs, prediction of chute cutoffs will probably always involve probabilistic assessment. Nonetheless, better models and calibration procedures must await more extensive observations on chute cutoffs. Even with neck cutoffs our ability to make detailed projections of the future

course of bend migration decreases rapidly with temporal separation of present and future (or past). This is even more problematic when chute cutoffs are involved. Only general relationships such as those shown in Figures 16 &17 are likely to be possible for predictions into the distant future. Nevertheless, such data may prove useful for assessing the age structure of floodplain forests, the relative abundance of different physical habitats, etc. Furthermore, the simulation models may be utilize to analyze the spatial structure of riverine habitats, including patch size and shape.

Examination of floodplain evolution predicted by the calibrated model (Figures 5 and 9-13) suggests that unrealistically long cutoffs occur occasionally. Inclusion of a small positive value of K_d would make such long cutoffs less likely.

Because the simulation model is spatially explicit, the simulation of the Yampa floodplain evolution could be made more realistic by incorporating less erodible valley walls (e.g., Figure 1) in the simulation. Similarly, spatially variable resistance of floodplain alluvium could be incorporated, either stochastically or based upon survey information or aerial photos. For example, old oxbow lakes filled with clayey alluvium may be more resistant to erosion than normal point bar deposits, so that mapping of old oxbow lakes could be used to constrain simulations. For examples see Howard (1996). Similarly, effects of man-made constraints such a revetments, bridge piers, artificial cutoffs, etc. could be incorporated.

During the course of this investigation we did not attempt to calibrate the floodplain deposition model. This could be done at a later time by the combination of two techniques. The first is dating of various floodplain locations by tree ring analysis and looking at the elevation of the floodplain as a function of age and distance from the channel. The second is using surveyed cross sections across point bars formed since 1938, because the aerial photo record permits assessment of floodplain age. The extent of infilling of oxbow lakes of known age can also be determined and used for calibration.

References

Howard, A. D., 1992, Modelling channel migration and floodplain development in meandering streams. In: *Lowland Floodplain Rivers*, P. A. Carling and G.E. Petts (eds.), Chichester, John Wiley & Sons, 1-42.

Howard, A.D., 1996, Modelling channel evolution and floodplain morphology. In: *Floodplain Processes*, M. G. Anderson, D.E. Walling, and P.D. Bates (eds.), Chichester, John Wiley & Sons, 15-62.

Howard, A.D. and Hemberger, A.T., 1991, Multivariate characterization of meandering, *Geomorphology*, **4**, 161-186.

Ikeda, S., Parker, G., and K. Sawaii, 1981, Bend theory of river meanders, 1, Linear development, *Journal of Fluid Mechanics*, **112**, 363-377.

Johanneson, J. and G. Parker, 1989, Linear theory of river meanders. In: *River Meandering*, S. Ikeda and G. Parker (eds.), Water Resources Monograph 12, American Geophysical Union, 103-126.

Figure Captions

Figure 1. Base map of the Yampa River near Hayden showing 1938 and 1989 channels.

Figure 2. Centerlines of the Yampa River from 1938 (solid) and 1989 (dashed) for a portion of the channel shown in Figure 1.

Figure 3. Temporal evolution of channel sinuosity (starting from a straight stream) when cutoffs are strongly controlled by the distance across the cutoff (the K_d parameter). Note that after full meandering is developed the sinuosity fluctuates through a narrow range.

Figure 4. Temporal evolution of channel sinuosity when the K_d parameter is assumed not to affect cutoff probability. Note the large excursions of sinuosity. See also Figure 15.

Figure 5. Representative centerlines for a simulation with 10,000 iterations starting from the 1938 Yampa River centerline. Note that the range of excursion of the channel around the initial channel location is generally limited to about 3 times the meander amplitude. Howard (1996) shows that meander belt width increases logarithmically with time in simulated meandering.

Figure 6. Temporal evolution of sinuosity for five simulations with K_c=0.015. Each simulation was seeded with a different random number for the probabilistic cutoff model. The simulations started from the 1938 planform and continued for 500 iterations (or about 1700 model years). Note the wide temporal variation in sinuosity and the divergence of the several simulations due to the probabilistic nature of the cutoffs.

Figure 7. Temporal evolution of sinuosity for five simulations with K_c=0.02. See Figure 6 for further explanation.

Figure 8. Temporal evolution of sinuosity for five simulations with K_c=0.025. See Figure 6 for further explanation.

Figures 9-13. Planform evolution for the 5 simulations whose temporal evolution of sinuosity is shown in Figure 7. Note the variation between the simulations in the location and timing of cutoffs.

Figure 14. "Goodness of fit" statistics for the simulations shown in Figures 9-13. Goodness of fit is measured by the mean and standard deviation of the separations between the simulated planforms (which started from the 1938 centerline) and the 1987 planform. The error in the fit generally decreases during the first 550 iterations, but then increases afterwards. This suggests that 550 'years' of the simulation model corresponds to the 51 years between 1938 and 1989.

Figure 15. Evolution of sinuosity for the 10000 iteration simulation shown in Figure 5. Note that sinuosity varies between about 1.2 to 2.2.

Figure 16. Graph of mean elevation and cumulative frequency of occurrence of floodplain area as a function of floodplain age for the simulation shown in Figure 5.

Figure 17. Graph of mean age, mean elevation, and cumulative frequency of occurrence of floodplain area as a function of distance from the final simulated channel for the simulation shown in Figure 5.

Yampa River In the Vicinity of Hayden, Colorado

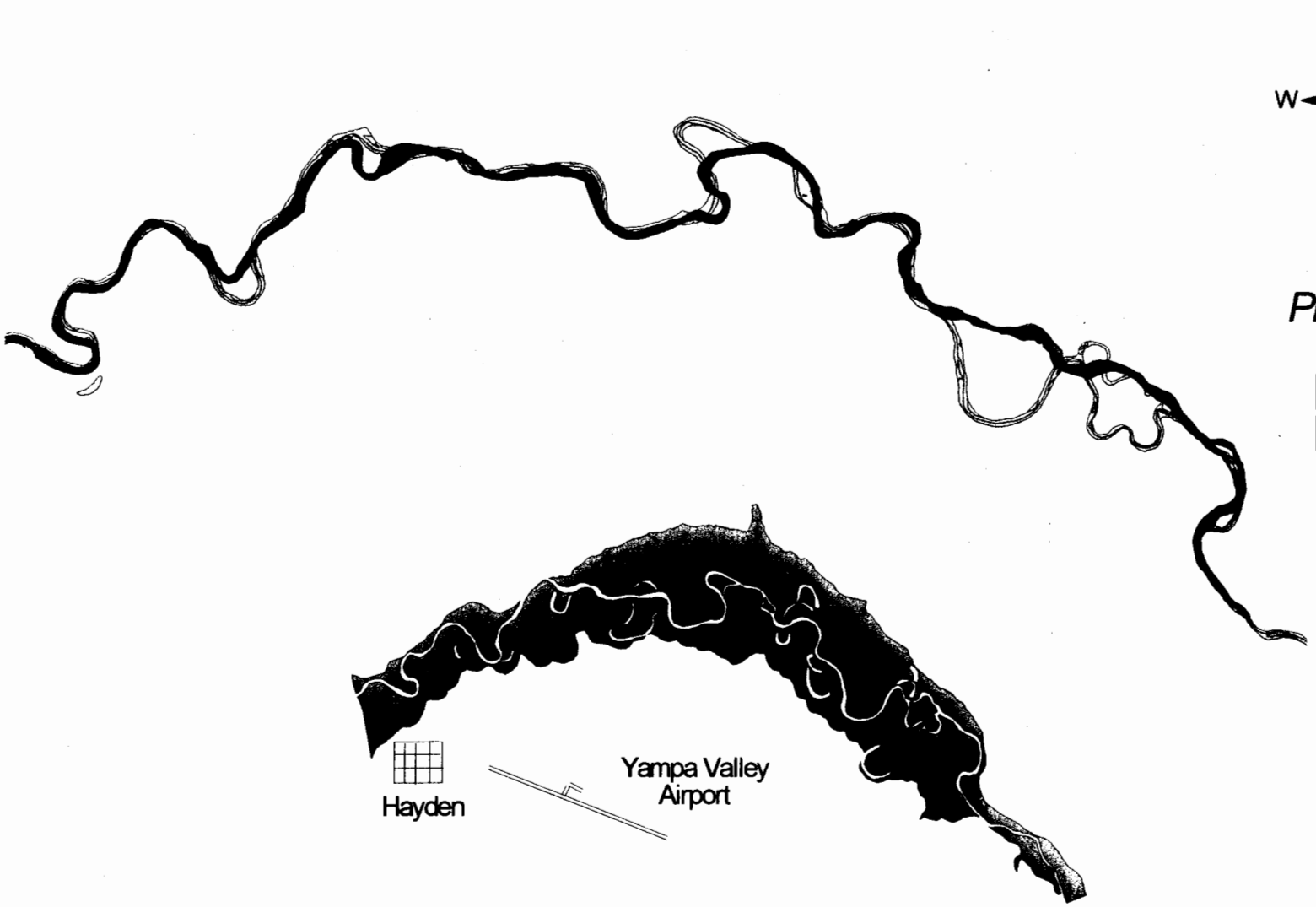

Map analysis created
by Eric Walden
University of Virginia
April 29, 1997

Data collected in the field
by Christina Ostendorf
mcostend@umt.net
1994-1995

Figure 1

YAMPA 1938 & 1989

H

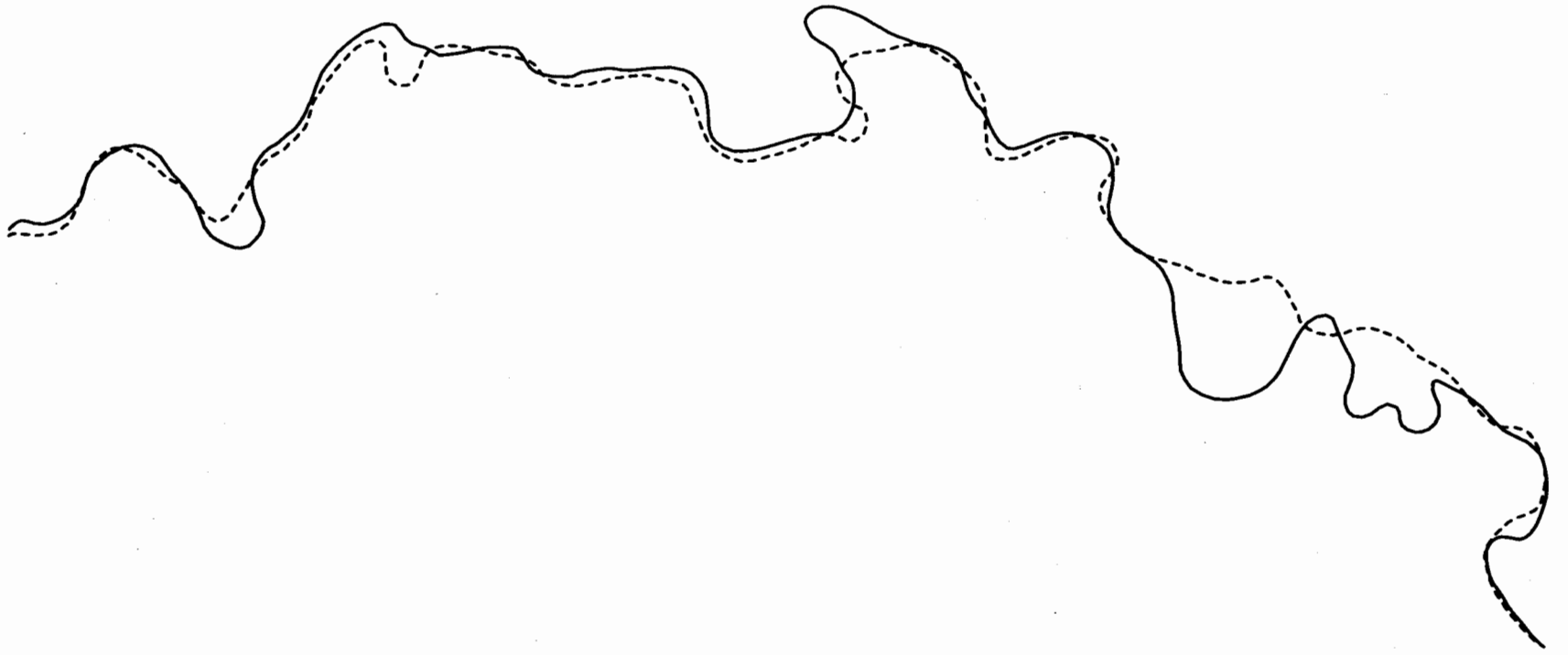

Figure 2

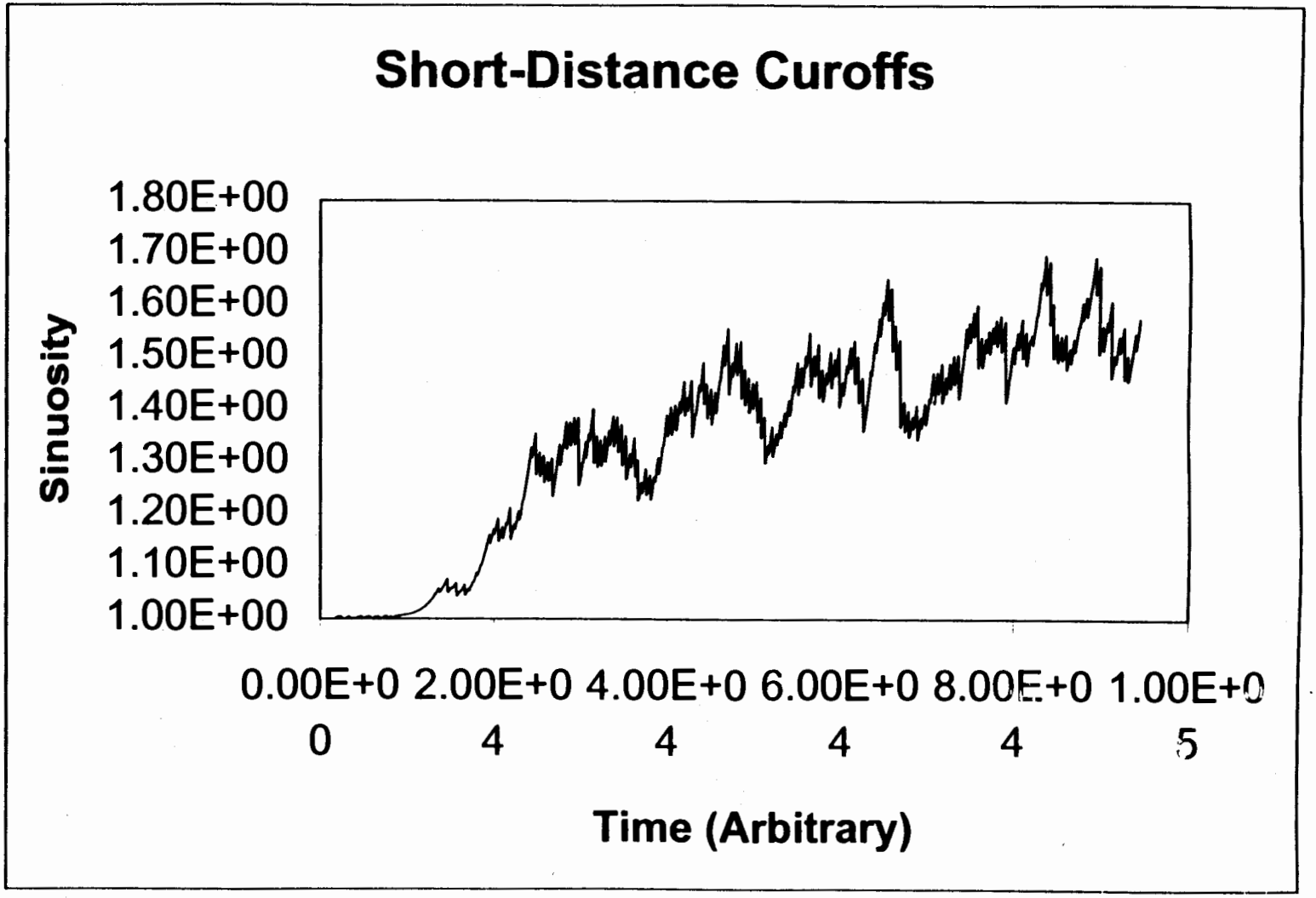
Short-Distance Curoffs
Sinuosity
1.80E+00
1.70E+00
1.60E+00
1.50E+00
1.40E+00
1.30E+00
1.20E+00
1.10E+00
1.00E+00
0.00E+0 2.00E+0 4.00E+0 6.00E+0 8.00E+0 1.00E+0
0 4 4 4 4 5
Time (Arbitrary)

Figure 3

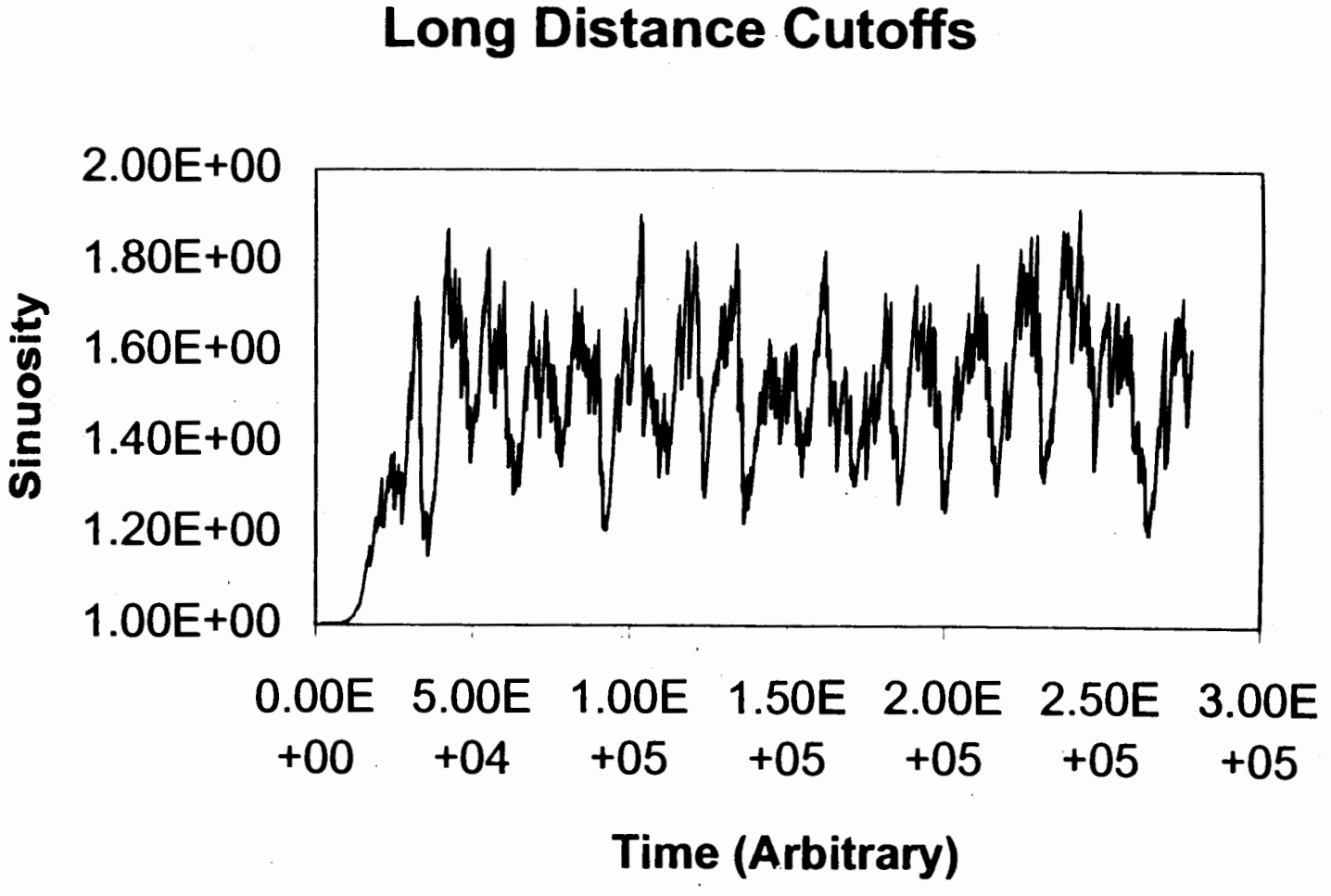
Long Distance Cutoffs
2.00E+00
1.80E+00
1.60E+00
1.40E+00
1.20E+00
1.00E+00
Sinuosity
0.00E +00
5.00E +04
1.00E +05
1.50E +05
2.00E +05
2.50E +05
3.00E +05
Time (Arbitrary)

Figure 4

Long Yampa Simulation

H

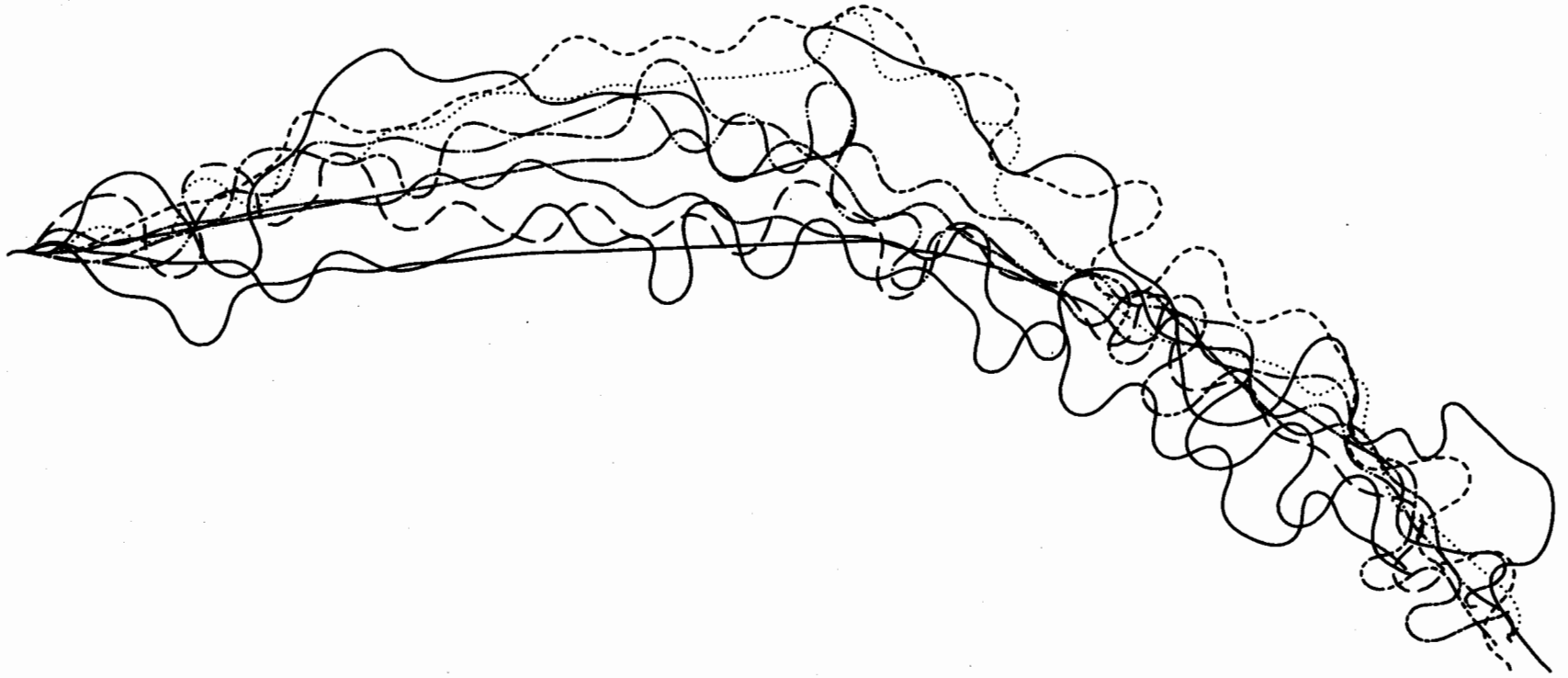

Figure 5

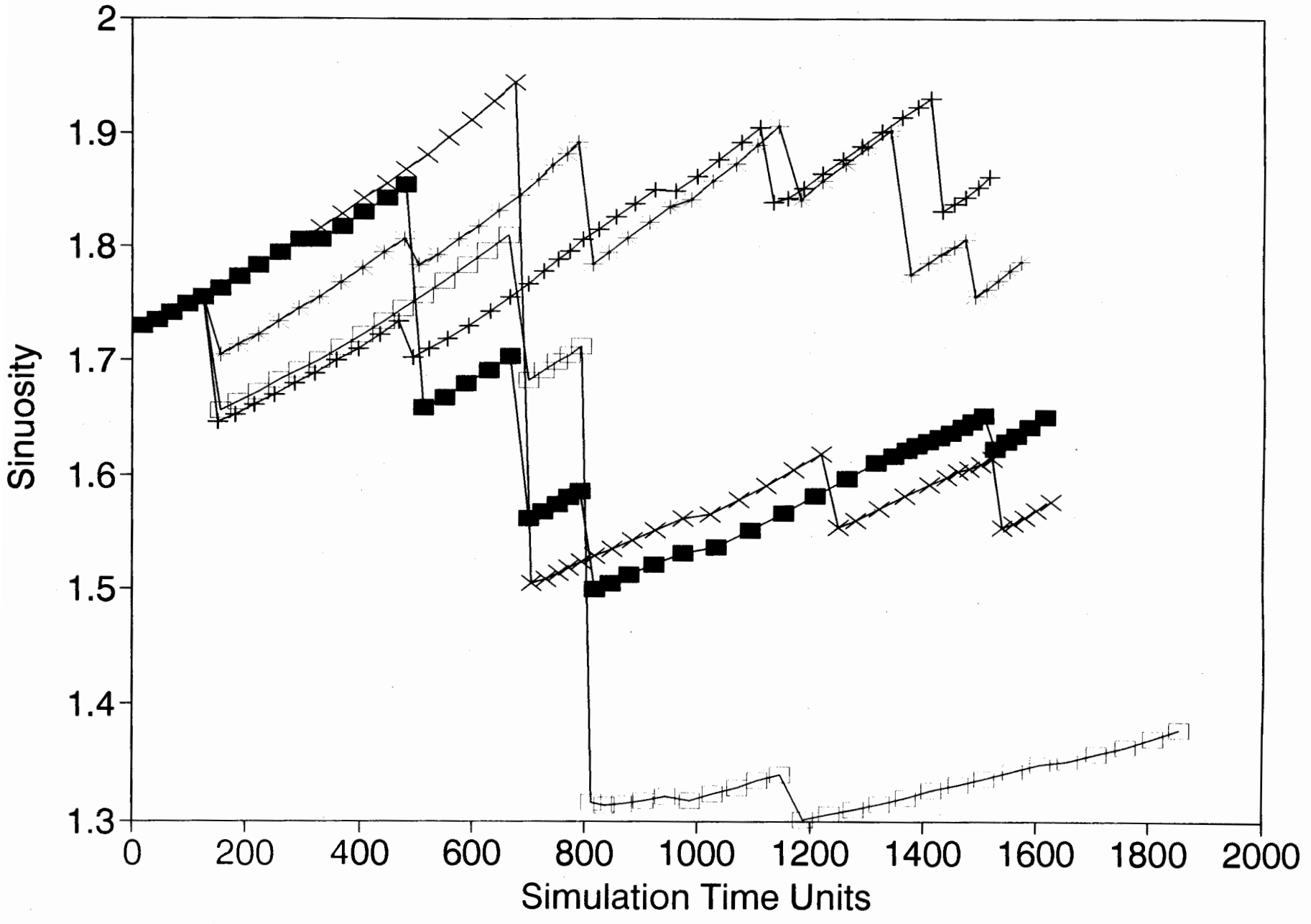
Chute Cutoff Factor = 0.015
Sinuosity
2
1.9
1.8
1.7
1.6
1.5
1.4
1.3
0
200
400
600
800
1000
1200
1400
1600
1800
2000
Simulation Time Units

Figure 6

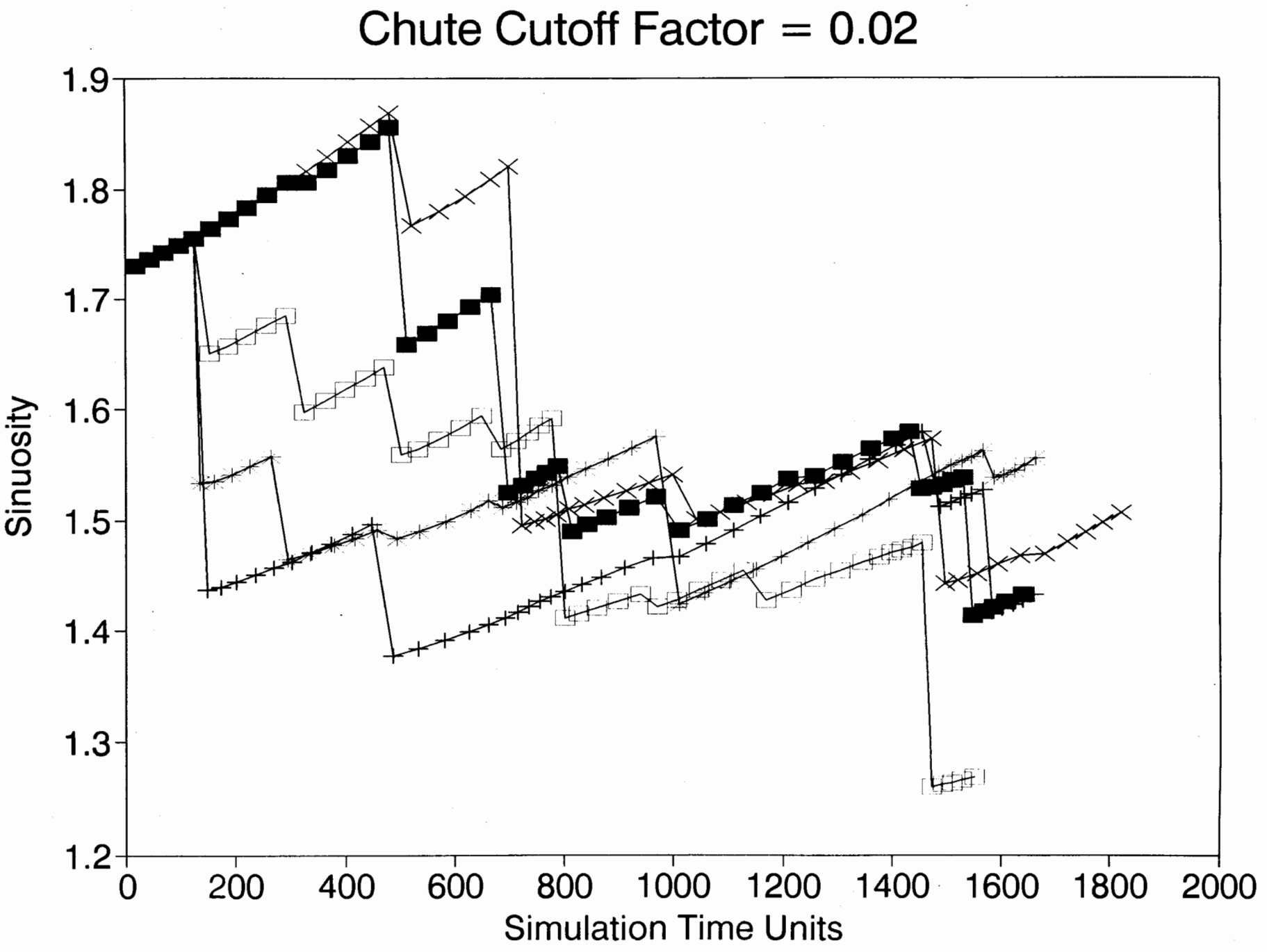
Chute Cutoff Factor = 0.02
Sinuosity
1.9
1.8
1.7
1.6
1.5
1.4
1.3
1.2
0
200
400
600
800
1000
1200
1400
1600
1800
2000
Simulation Time Units

Figure 7

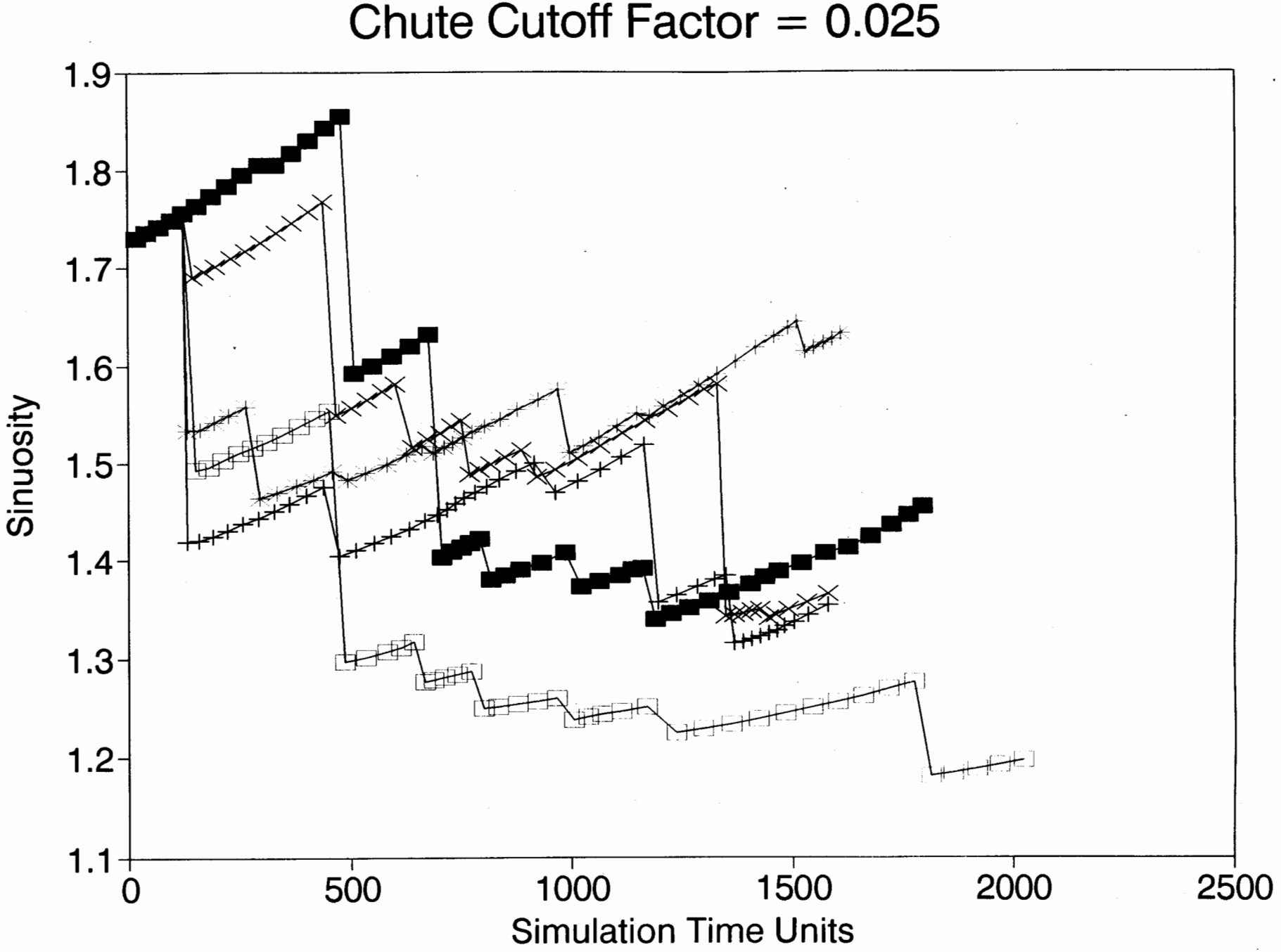
Chute Cutoff Factor = 0.025
Sinuosity
1.9
1.8
1.7
1.6
1.5
1.4
1.3
1.2
1.1
0
500
1000
1500
2000
2500
Simulation Time Units

Figure 8

Factor = 0.02 Run #1

H

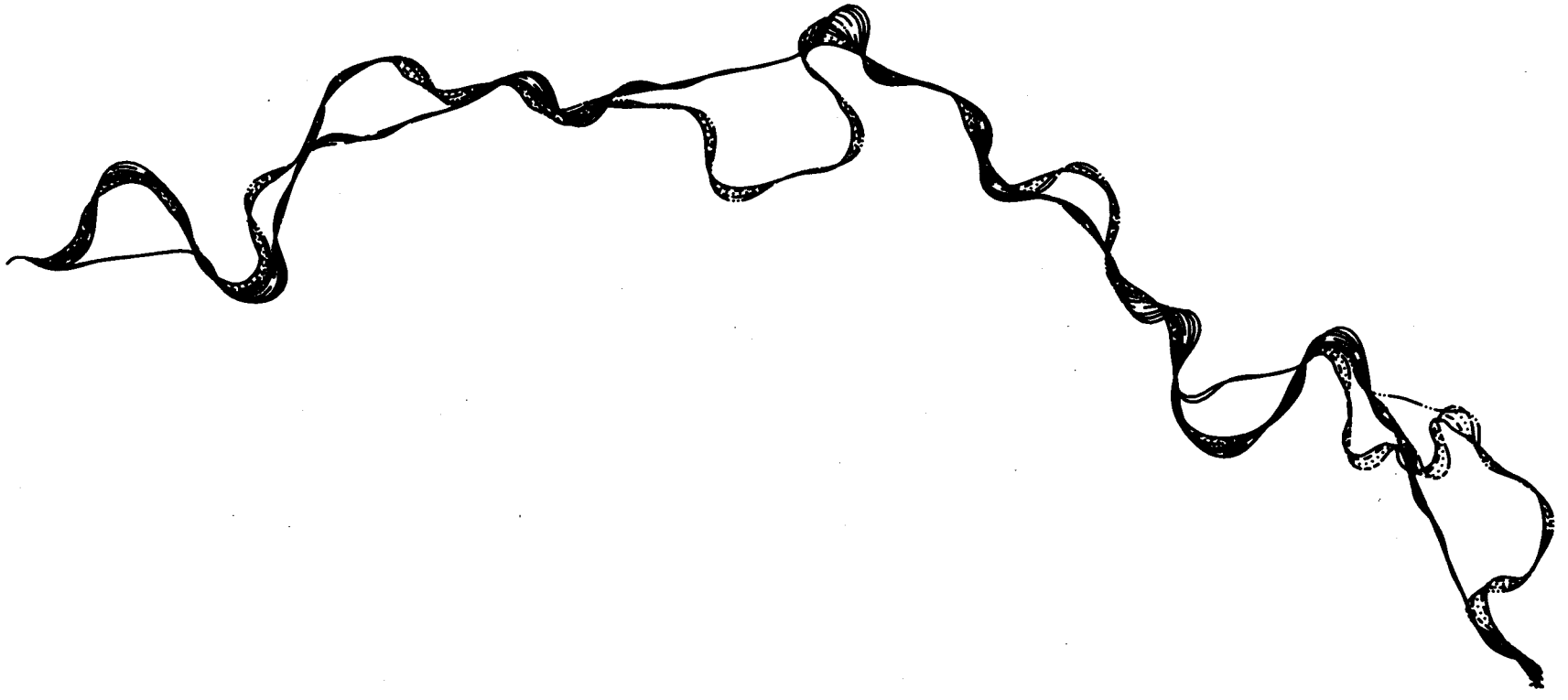

Figure 9

Factor = 0.02 Run #2

H

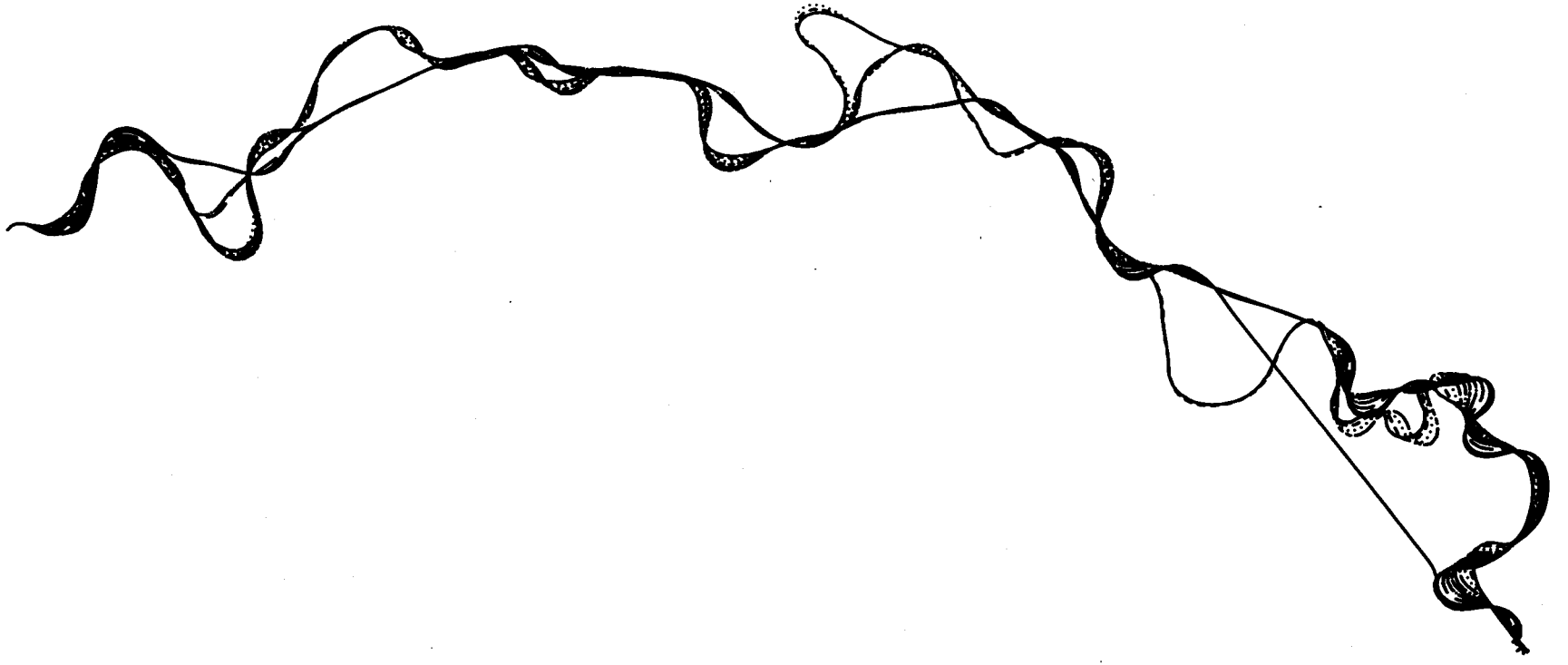

Figure 10

Factor = 0.02 Run #3

H

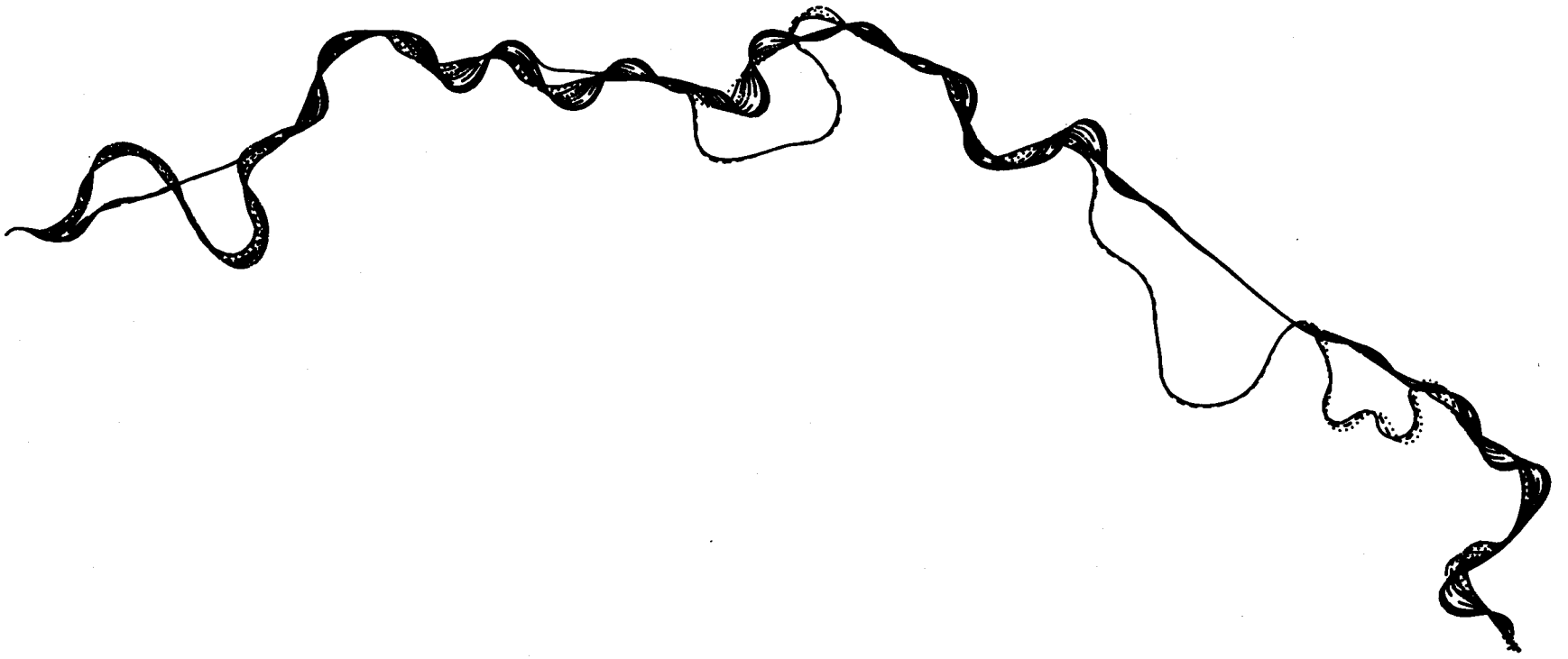

Figure 11

Factor = 0.02 Run #4

H

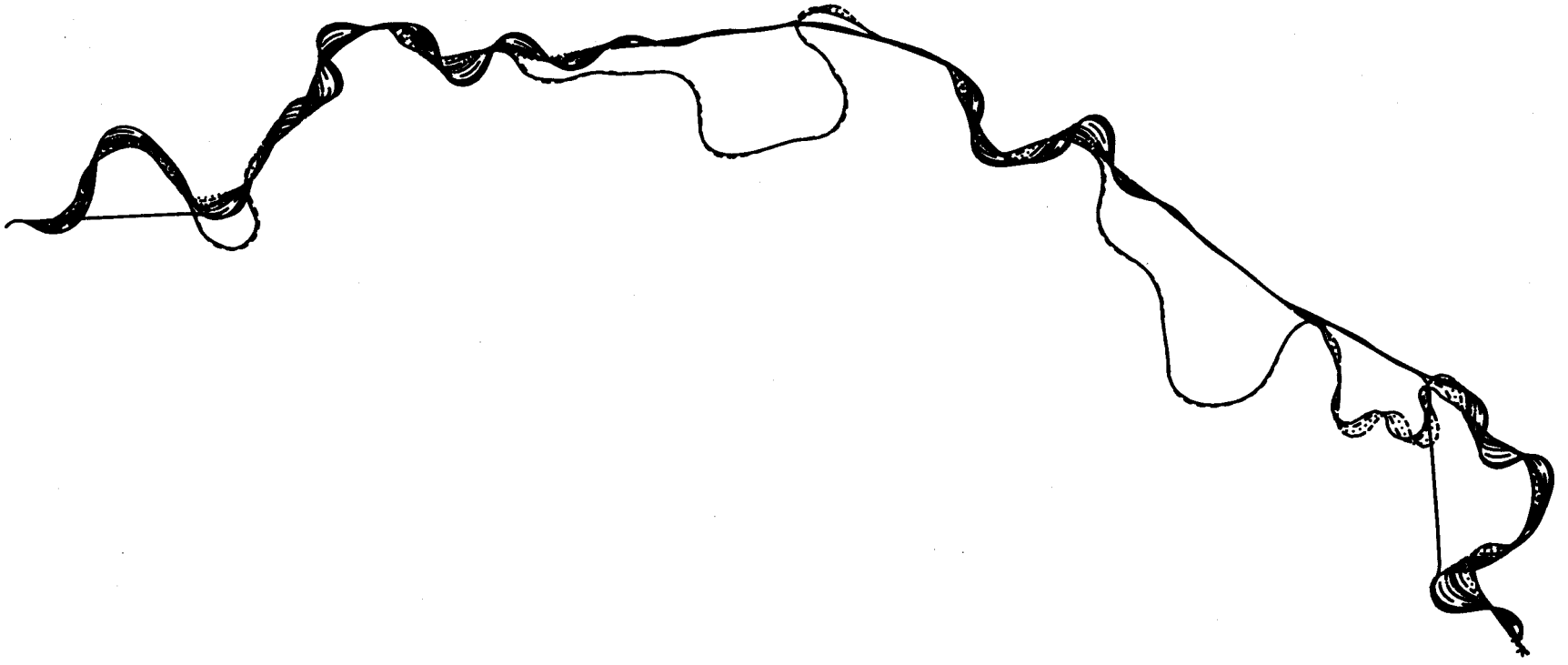

Figure 12

Factor = 0.02 Run #5

H

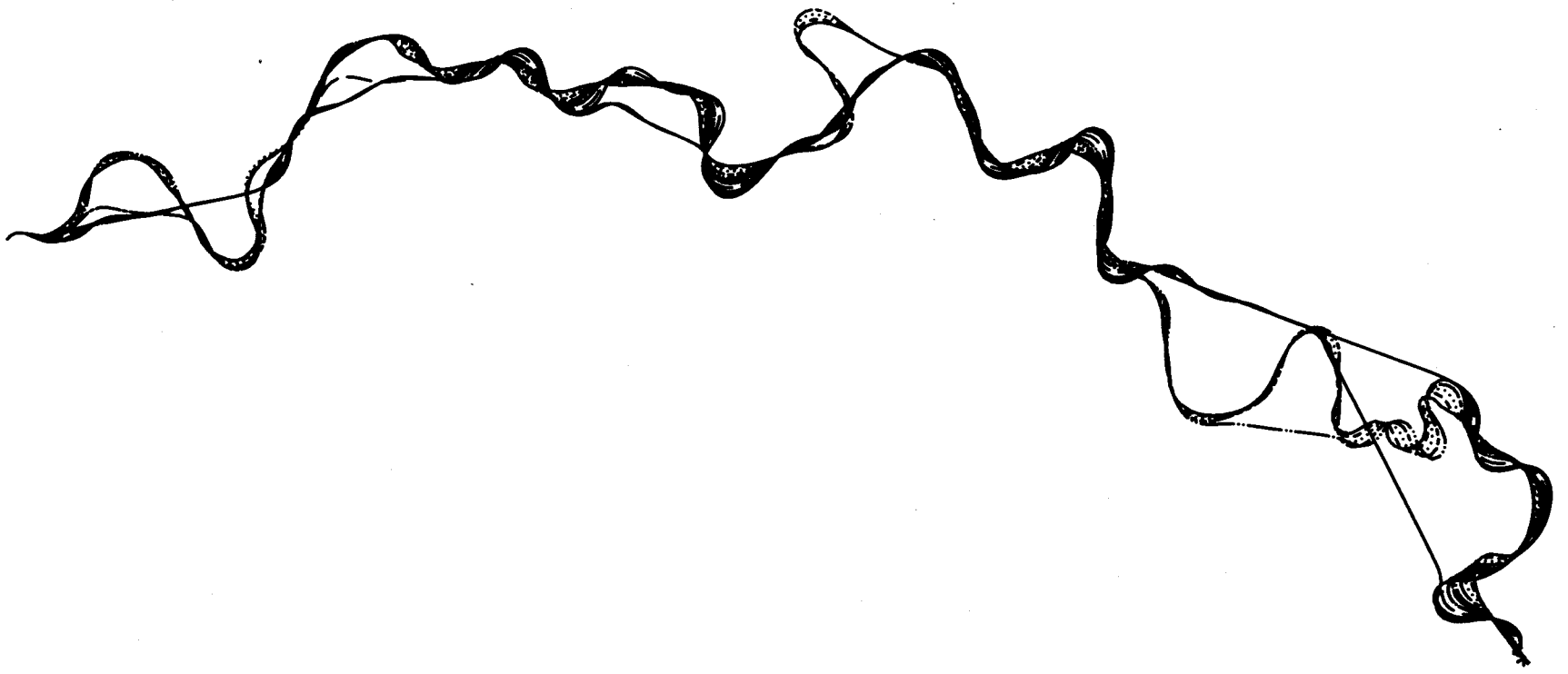

Figure 13

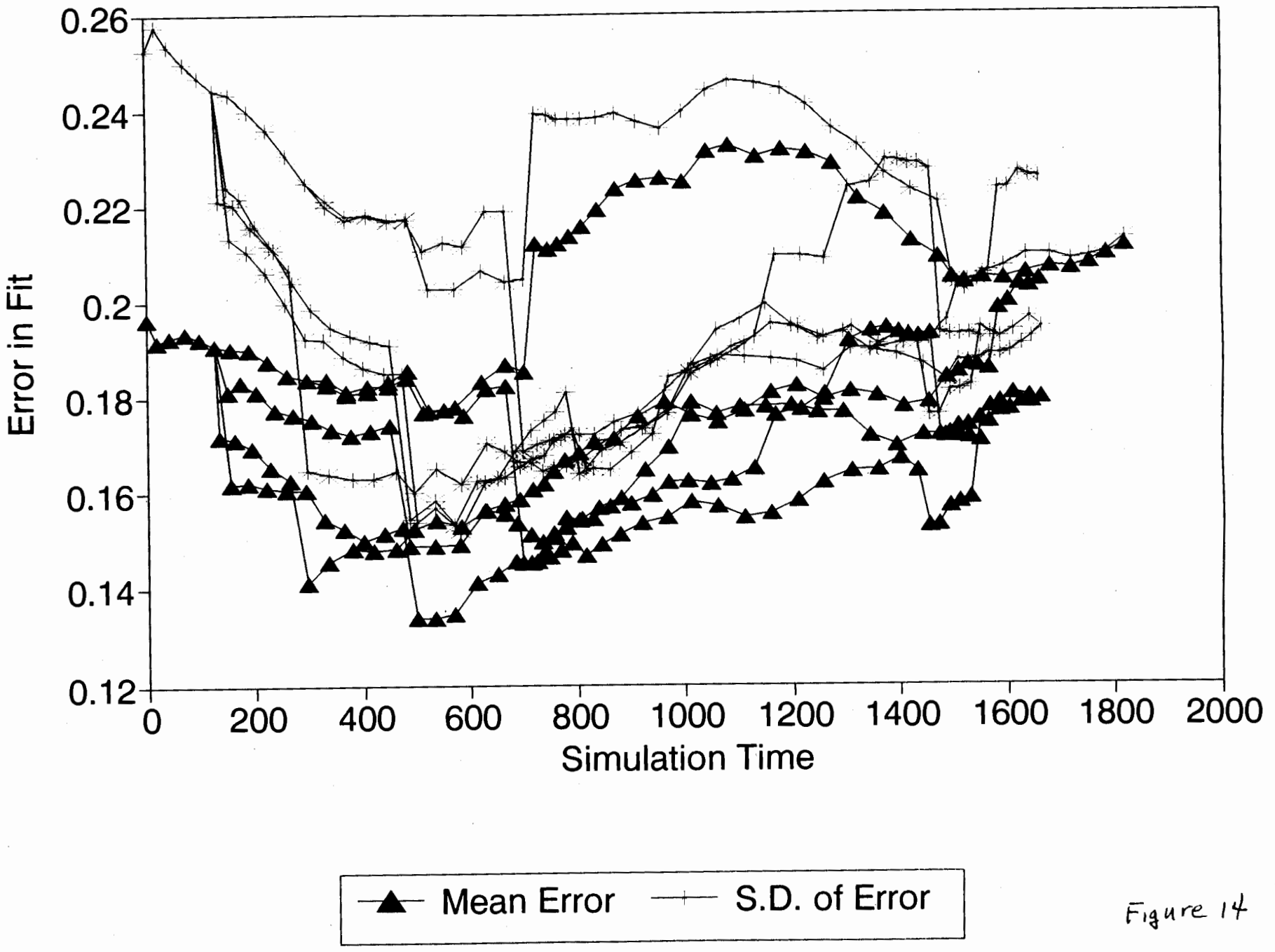
Measures of Goodness of Fit
Error in Fit
0.26
0.24
0.22
0.2
0.18
0.16
0.14
0.12
0
200
400
600
800
1000
1200
1400
1600
1800
2000
Simulation Time
Mean Error
S.D. of Error

Figure 14

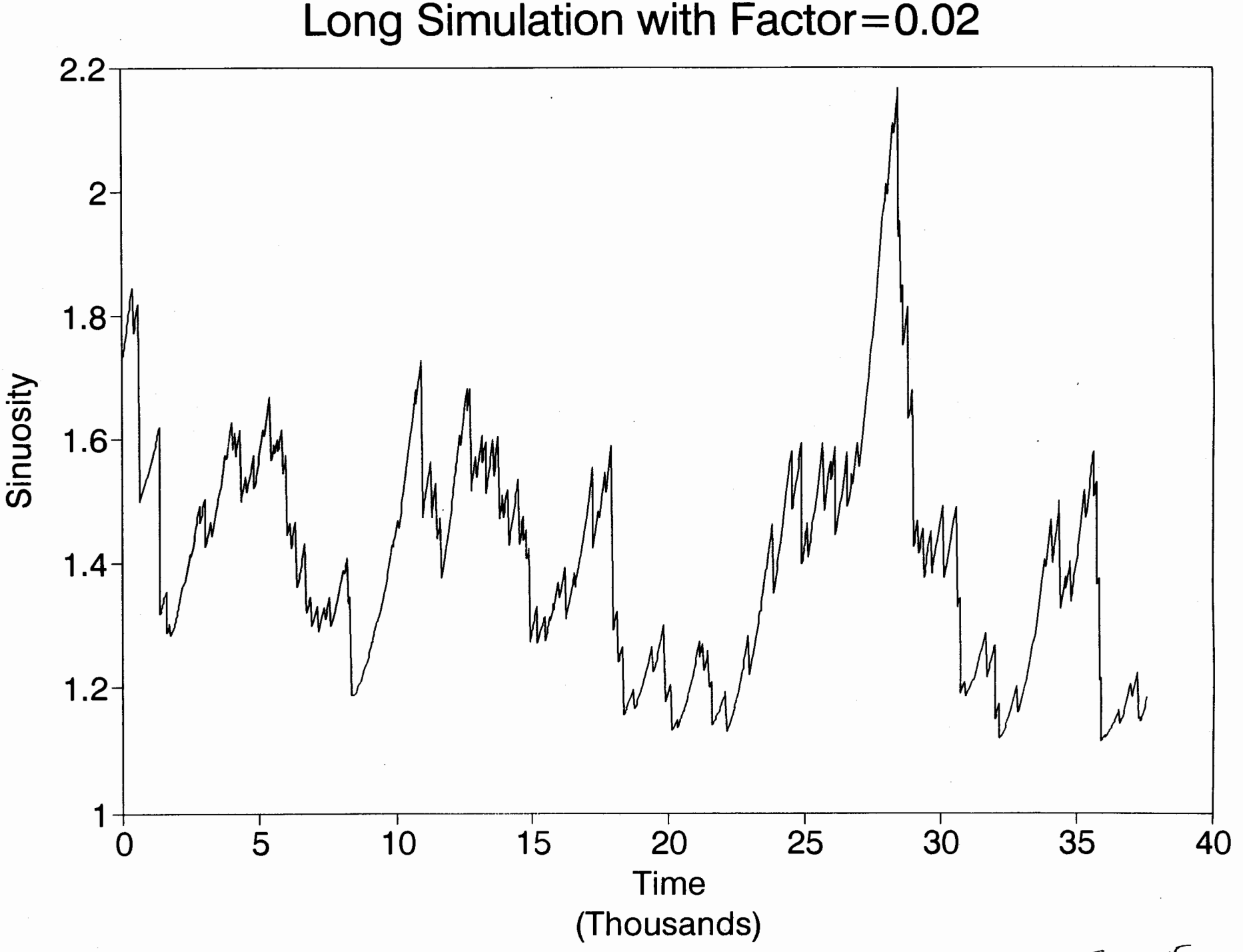
Long Simulation with Factor=0.02
Sinuosity
2.2
2
1.8
1.6
1.4
1.2
1
0
5
10
15
20
25
30
35
40
Time
(Thousands)

Figure 15

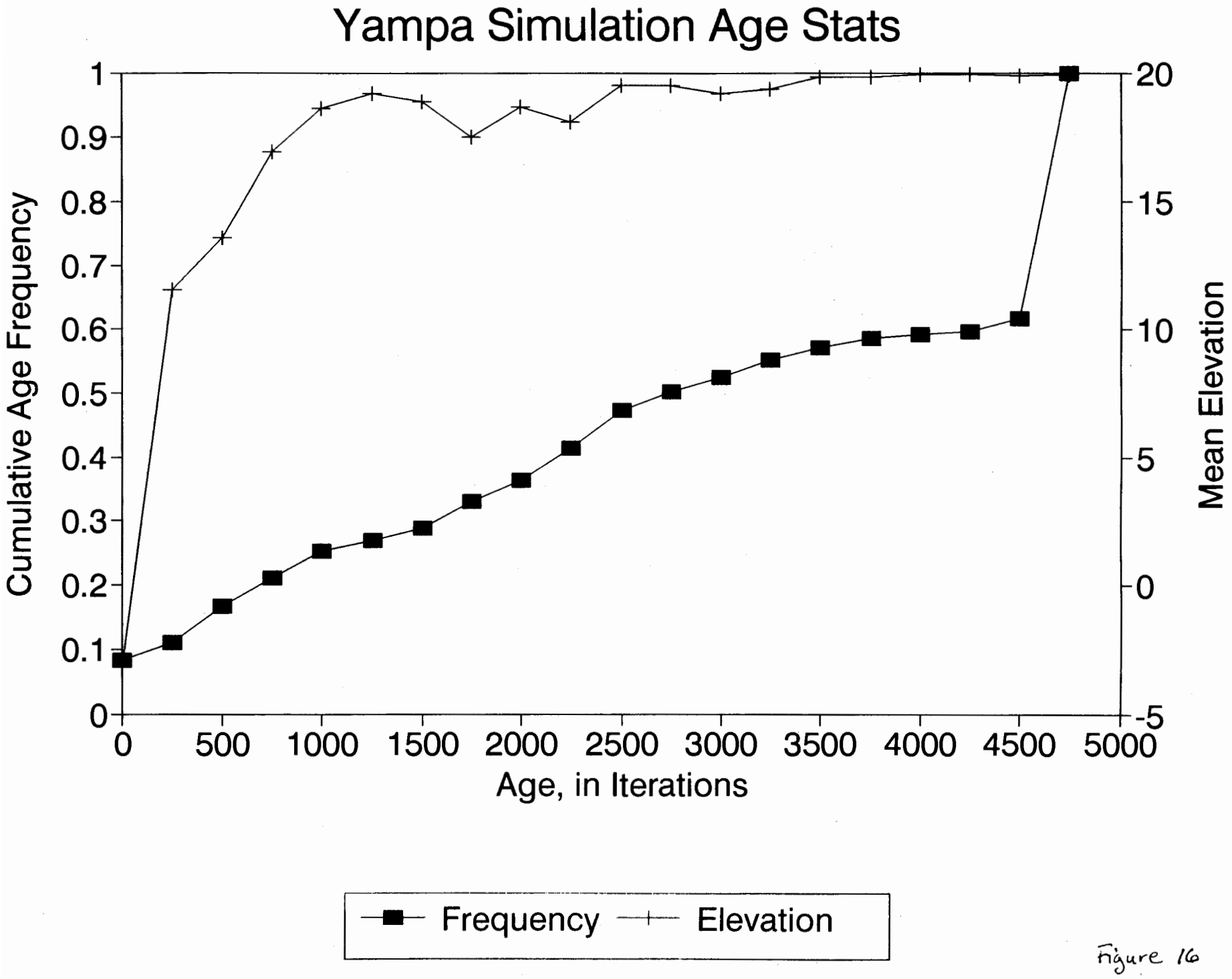
Yampa Simulation Age Stats
Cumulative Age Frequency
Mean Elevation
Age, in Iterations
0
0.1
0.2
0.3
0.4
0.5
0.6
0.7
0.8
0.9
1
-5
0
5
10
15
20
0
500
1000
1500
2000
2500
3000
3500
4000
4500
5000
Frequency
Elevation

Figure 16

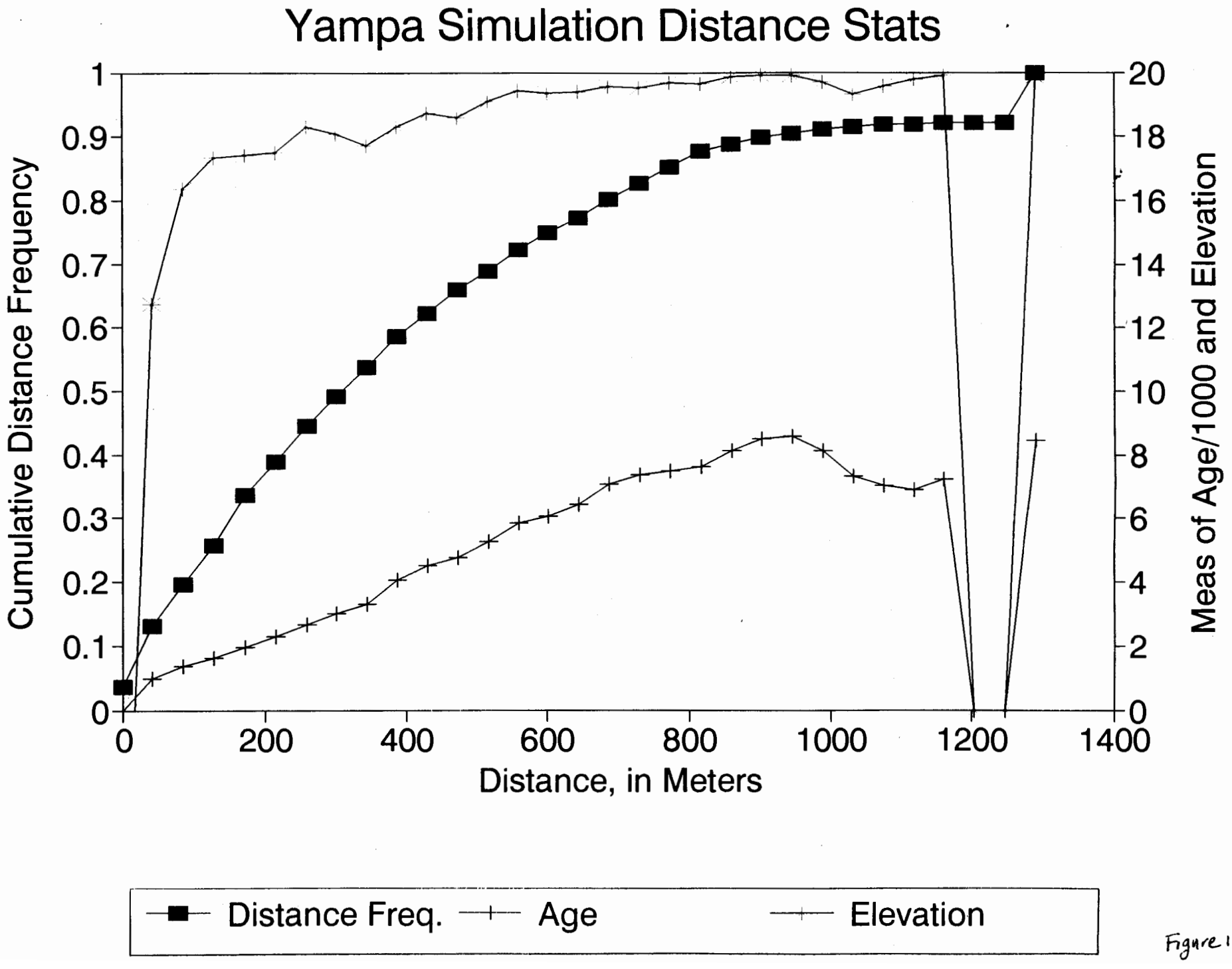
Yampa Simulation Distance Stats
Cumulative Distance Frequency
Meas of Age/1000 and Elevation
Distance, in Meters
0
0.1
0.2
0.3
0.4
0.5
0.6
0.7
0.8
0.9
1
0
2
4
6
8
10
12
14
16
18
20
0
200
400
600
800
1000
1200
1400
Distance Freq.
Age
Elevation

Figure 17